

Cavity Quantum Electrodynamics Enables para- and ortho-Bromination of Nitrobenzene

Braden M. Weight,^{*,†} Daniel J. Weix,[‡] Zachary J. Tonzetich,[¶] Todd D. Krauss,^{§,||} and Pengfei Huo^{*,§,||}

[†]*Department of Physics and Astronomy, University of Rochester, Rochester, NY 14627, U.S.A.*

[‡]*Department of Chemistry, University of Wisconsin-Madison, Madison, WI 53706, U.S.A.*

[¶]*Department of Chemistry, University of Texas at San Antonio, San Antonio, TX 78249, U.S.A.*

[§]*Department of Chemistry, University of Rochester, Rochester, NY 14627, U.S.A.*

^{||}*The Institute of Optics, Hajim School of Engineering, University of Rochester, Rochester, NY 14627, U.S.A.*

E-mail: bweight@ur.rochester.edu; pengfei.huo@rochester.edu

Abstract

Coupling molecules to a quantized radiation field inside an optical cavity has shown great promise to modify chemical reactivity. While most ongoing work is leveraging resonance effects between the molecular transitions and the frequency of the cavity, the ground state can also be modified through non-resonant effects dominated by dipole self-energy contributions. In this work, we predict that the ground state selectivity of the bromination of nitrobenzene can be fundamentally changed by strongly coupling to the cavity, generating the ortho- or para-substituted products. These are products that one does not obtain from the same reaction outside the cavity. We use the recently developed *ab initio* polariton chemistry approach and theoretically compute the relative energies of the cationic Wheland intermediates, which indicates the kinetically preferred bromination site. We have further provided an analysis of the ground state electron density difference between inside and outside cavity, and we demonstrate how coupling to the cavity can change the charge distribution which leads to different bromination sites.

Introduction

Coupling molecules to a quantized radiation field inside an optical cavity creates a set of photon-matter hybrid states, called polaritons. These polariton states have shown great promise to change chemical reaction kinetics. In one direction, collective couplings between the electronic excited state with the photonic states inside an optical cavity have been shown to enhance¹ or suppress² photochemical isomerization reactions. In another direction where collectively coupled vibrational excitations with the photonic excitations in microcavities, commonly referred to as vibrational strong coupling (VSC), has demonstrated that chemical kinetics can be enhanced^{3,4} or suppressed.⁵⁻⁷ In these two collective coupling regimes, the kinetics of the reactions are changed, but there is no new type of product generated compared to the same reactions outside the cavity.

In a new direction, recent theoretical investigations have suggested that the *ground state* of a molecular system can be significantly modified by coupling to a cavity photon mode with a photon frequency in the *electronic excitation range*.⁸⁻¹⁵ In particular, it has been shown that the cavity can modify the endo/exo selectivity of Diels-Alder reactions,¹⁴ modify the ground state proton transfer reactions barriers and driving forces,^{13,16} and selectively control the product regiochemistry in a model Huisgen cycloaddition.¹⁷ Note that the cavity frequency in these studies is chosen to be in the range of electronic excitation (in terms of energy, on the order of eV), thus different than the re-

cently explored vibrational strong coupling (VSC) regime.^{5,7} This new type of the cavity-modified chemistry does not require the usual resonance effects of light-matter interactions (*i.e.*, frequency matching between light and matter excitations), and the cavity can directly modify the ground state of the hybrid system, hence referred to as the quantum vacuum fluctuation modified chemistry^{13,14} This direction offers the potential to fundamentally change reaction mechanisms and generate new products that are otherwise not available. Such a single molecule-cavity strong coupling regime is also within the reach of recent experiments using a plasmonic nano-cavity.¹⁸

To conceptually understand these recently proposed ground state modifications due to cavity vacuum fluctuations,^{13,14,19} let us consider the quantum mechanical description of the molecule-cavity hybrid system using the Pauli-Fierz Hamiltonian in the dipole gauge^{19–21}

$$\hat{H}_{\text{PF}} = \hat{H}_{\text{el}} + \hat{H}_{\text{ph}} + \omega_c A_0 \hat{\boldsymbol{\mu}} \cdot \hat{\mathbf{e}}(\hat{a}^\dagger + \hat{a}) + \omega_c A_0^2 (\hat{\boldsymbol{\mu}} \cdot \hat{\mathbf{e}})^2, \quad (1)$$

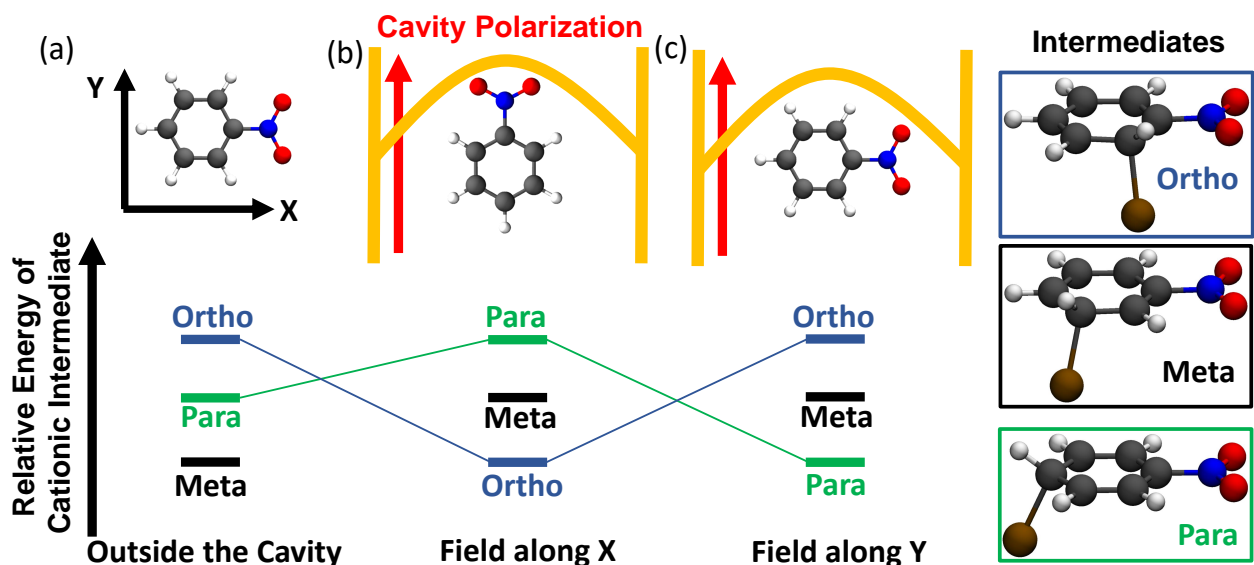
where \hat{H}_{el} is the electronic Hamiltonian under the Born-Oppenheimer approximation (*i.e.*, without the nuclear kinetic energy operator), $\hat{H}_{\text{ph}} = \omega_c \hat{a}^\dagger \hat{a}$ is the Hamiltonian of the cavity field, \hat{a}^\dagger and \hat{a} are the raising and lowering operators of the cavity field, $\hat{\mathbf{e}}$ is a unit vector indicating the field polarization direction, and $\hat{\boldsymbol{\mu}}$ is the dipole operator of the molecule. The light-matter coupling strength is expressed as

$$A_0 = \sqrt{\frac{1}{2\omega_c \varepsilon \mathcal{V}}}, \quad (2)$$

where \mathcal{V} is the effective mode volume of the cavity, and ε is the permittivity inside the cavity. Through light-matter coupling terms, various photon-dressed electronic states will be coupled to each other. For example, $|\psi_g, 1\rangle \equiv |\psi_g\rangle \otimes |1\rangle$ (the ground electronic state with 1 photon) and $|\psi_e, 0\rangle \equiv |\psi_e\rangle \otimes |0\rangle$ (an excited electronic state with 0 photons) will couple through $\langle \psi_g, 1 | \hat{\boldsymbol{\mu}} \cdot \hat{\mathbf{e}}(\hat{a}^\dagger + \hat{a}) | \psi_e, 0 \rangle = \mu_{ge} \langle 1 | (\hat{a}^\dagger + \hat{a}) | 0 \rangle$, where μ_{ge} is the transition dipole between the ground state and excited state projected along the $\hat{\mathbf{e}}$ direction. When the energy of these two basis states become close, the $|\psi_g, 1\rangle$ and $|\psi_e, 0\rangle$ states hybridize, leading to the formation of excited polariton states. This is the typical resonant light-matter coupling induced hybridization and generating new eigenstates, and polaritons.

The direct modifications to the polariton ground states, on the other hand, are caused by two types of couplings^{19,20,22} in the Hamiltonian: (i) off-resonance light-matter couplings (third term in Eq. 1) through the ground state permanent dipole and transition dipoles between the ground and excited states, and (ii) the dipole self-energy (final term in Eq. 1). For example, in (i), $|\psi_g, 0\rangle$ will couple to $|\psi_g, 1\rangle$ state through $\langle \psi_g, 0 | \hat{\boldsymbol{\mu}}(\hat{a}^\dagger + \hat{a}) | \psi_g, 1 \rangle = \mu_{gg} \langle 0 | (\hat{a}^\dagger + \hat{a}) | 1 \rangle$, and $|\psi_g, 1\rangle$ will couple to $|\psi_e, 0\rangle$ through $\langle \psi_e, 0 | \hat{\boldsymbol{\mu}}(\hat{a}^\dagger + \hat{a}) | \psi_g, 1 \rangle = \mu_{ge} \langle 0 | (\hat{a}^\dagger + \hat{a}) | 1 \rangle$. Note that there may be many such electronic excited states ψ_e that contribute to the ground state through this term. In (ii), the dipole self-energy term allows for extensive coupling through the square of the electronic dipole matrix $(\hat{\boldsymbol{\mu}} \cdot \hat{\mathbf{e}})^2 \equiv \hat{\mu}^2$ where we denote $\hat{\mu}$ as the projection of $\hat{\boldsymbol{\mu}}$ along the cavity polarization direction $\hat{\mathbf{e}}$. The matrix elements between the ground state $|\psi_g\rangle$ and any electronic state $|\psi_\alpha\rangle$ due to the DSE coupling can be expressed as $\langle \psi_g | \hat{\mu}^2 | \psi_\alpha \rangle = \sum_\gamma \mu_{g\gamma} \mu_{\gamma\alpha}$, where α and γ include the ground and excited electronic states. The direct coupling (i) is responsible for the accumulation of photons in the ground state⁸ while the dipole self-energy (ii) is largely responsible for the modifications to the ground state energy.²³ Through these non-resonance type of light-matter interactions, the cavity can directly modify the ground state of the hybrid system (which is beyond the prediction of the simple Jaynes-Cummings model²⁴) and is thus referred to as quantum vacuum fluctuation modified chemistry^{13,14}

In this work, we aim to demonstrate that the strong coupling between molecule and cavity can fundamentally change the reaction outcome of the bromination of nitrobenzene in its ground state. This is a textbook reaction,²⁵ where the *only* observed product is the *meta*-substitution product; the ortho-substituted or para-substituted products can not be observed experimentally. This has been well-explained due to the relative stability of the catatonic active complex $\text{PhNO}_2\text{-Br}^+$, for example, using the resonance structure analysis. We apply the recently developed *ab initio* polariton chemistry approach,¹⁶ and theoretically demonstrate that one can fundamentally change the selectivity of this reaction, making possible the ortho- or para-substituted products by coupling this reaction inside an optical cavity. We have further provided an analysis of how coupling to the cavity can change the charge distribution of the catatonic active complex which causes the change of the pre-



Scheme 1: (a, top) The nitrobenzene molecule, a reactant in the bromination reaction, with **X** and **Y** direction in the plane of benzene ring and the **Z** axis perpendicular to the benzene ring. (b, top) and (c, top) indicates the inside the cavity in the (b) **X**-orientation and (c) **Y**-orientation with respect to the cavity polarization (red arrow). (a-c, bottom) A schematic representations of the potential energy surfaces for the bromination of nitrobenzene, where the intermediate species' energies (assumed to be the energy of the local minimum of the positively charged species outside the cavity) are tunable inside the cavity depending on the orientation of the molecule with respect to the cavity polarization. (a, bottom) Outside the the cavity, only the meta intermediate (black) is formed. The cavity allows selective bromination of the (b, bottom) ortho intermediate (blue) in the **X**-polarized case and (c, bottom) para intermediate (green) in the **Y**-polarized case. In the absence of cavity, the (a) meta position is experimentally and theoretically predicted. The right column presents the optimized intermediate geometries of the three possible $[\text{C}_6\text{H}_5\text{NO}_2\text{Br}]^+$ species.

ferred bromination site. As such, strong couplings between molecules inside the cavity offer a promising tool¹² to fundamentally change the outcome of a known chemical reactions, making an otherwise impossible product possible.

Results and Discussions.

The change of the selectivity of a bromination reaction can be achieved by coupling the nitrobenzene molecule to an optical cavity (see Scheme 1). In this work, we focus on the cavity modification of the energies of positively charged reaction intermediates $\text{PhNO}_2\text{-Br}^+$. This intermediate is well accepted as the quasi-stable intermediate species in the kinetics of the bromination of nitrobenzene, and the site selectivity of halogenations of aryl species is largely dictated by this intermediate.²⁵ Outside the cavity, the meta-intermediate is the most stable (see Scheme 1a,d) for nitrobenzene and provides nearly perfect regioselectivity due to a favorable resonance structure and the para- and ortho-substituted products can not be observed due to high-energy resonant structures. (For pos-

sible resonance structures for intermediates with different substitution sites, see Fig. S1 in the **Supporting Information**).

Scheme 1 presents the nitrobenzene reactant molecule (a) outside the cavity as well as coupled inside the cavity with the cavity polarization vector \hat{e} along the (b) **X**-direction or (c) **Y**-direction of the molecule, where these directions are defined in panel (a). Our *ab initio* calculations of the reactive intermediates suggest that outside the cavity (Scheme 1d), the meta-substituted intermediate (black line) is energetically more stable than the ortho-substituted (green line) and the para-substituted (blue line), leading to the meta-substituted product outside the cavity. The relative energies of different intermediates are changed by coupling the molecule to the cavity. A more stable ortho-substituted intermediate is formed if the cavity polarization is along the **X**-direction of the molecule (Scheme 1e) while the para substituent becomes stabilized if the cavity polarization is along the **Y**-direction (Scheme 1f).

Fig. 1 presents the relative stability of the three positively charged intermediate species when cav-

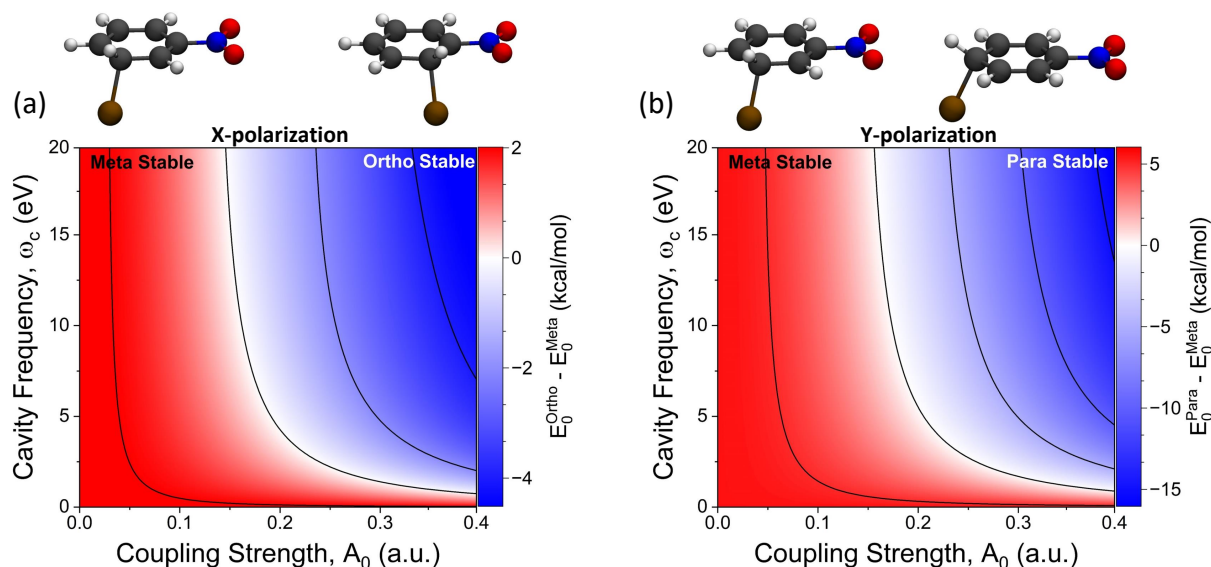


Figure 1: (a) Relative energy $E_0^{\text{Ortho}}(\mathbf{R}) - E_0^{\text{Meta}}(\mathbf{R})$ of the polaritonic ground states between the ortho-PhNO₂-Br⁺ and the meta-PhNO₂-Br⁺ cationic intermediate species, as a function of the light-matter coupling strength A_0 and the cavity frequency ω_c . The cavity polarization is $\hat{\mathbf{e}} = \hat{X}$ (see Scheme. 1). (b) The same plot for $E_0^{\text{Para}}(\mathbf{R}) - E_0^{\text{Meta}}(\mathbf{R})$, the relative energy between the para-PhNO₂-Br⁺ and the meta-PhNO₂-Br⁺ cationic intermediate species where the cavity polarization is $\hat{\mathbf{e}} = \hat{Y}$. The color scales indicate the relative energy with red showing thermodynamic favorability for the meta-substituted cation and blue for the other. The structures for the meta, ortho, and para intermediate species are shown above the figures.

ity (a) polarized along the $\hat{\mathbf{e}} = \mathbf{X}$ direction (primary axis of the molecule) or (b) polarized along the $\hat{\mathbf{e}} = \mathbf{Y}$ direction. The relative energy difference is reported as (a) the polaritonic ground states between the ortho-PhNO₂-Br⁺ and the meta-PhNO₂-Br⁺ cationic intermediate species, denoted as $E_0^{\text{Ortho}}(\mathbf{R}) - E_0^{\text{Meta}}(\mathbf{R})$ and (b) $E_0^{\text{Para}}(\mathbf{R}) - E_0^{\text{Meta}}(\mathbf{R})$, computed using Pauli-Fierz (PF) quantum electrodynamic (QED) Hamiltonian, with the linear-response time-dependent density functional (TD-DFT) approach as the input for the electronic excited state energies and dipole matrix elements.¹⁶ The theoretical details are provided in the **Theoretical Methods** section.

For outside the cavity case, which corresponds to the $A_0 = 0$ and $\omega_c = 0$ case (bottom left corner of Fig. 1a and Fig. 1b), one can see that the meta-substituted intermediate species is thermodynamically stable compared to the ortho- and para-species by roughly 2 and 5 kcal/mol, respectively. Coupling this intermediate inside the cavity, we find that the energy of the ortho- and para-substituted intermediate can have lower energy than the meta-substituted species under a range of coupling strength A_0 and cavity frequency ω_c .

Fig.1a presents the relative energetic stability of

the meta and ortho cationic intermediate species as $E_0^{\text{Ortho}}(\mathbf{R}) - E_0^{\text{Meta}}(\mathbf{R})$ inside the cavity with the cavity polarization along the \hat{X} -direction. For $\omega_c > 2.5$ eV and coupling strength $A_0 > 0.2$ a.u., the relative stability of the meta- and the ortho-substituted intermediates changes. Thus, inside the cavity, the ortho-substituted intermediate has a more stable energy, up to ~ 4 kcal/mol at the cavity frequency $\omega_c = 20.0$ eV and light-matter coupling strength $A_0 = 0.4$ a.u.

Fig.1b presents the relative energetics of the meta- and para-substituted intermediate species when the cavity polarization is along the \hat{Y} -direction (in the plane of the benzene ring). Here, the cavity induces stabilization of the para species in comparison to the meta by roughly ~ 15 kcal/mol at the largest values of cavity frequency $\omega_c = 20.0$ eV and light-matter coupling strength $A_0 = 0.4$ a.u. For comparison, room temperature thermal energy is $k_B T \approx 0.58$ kcal/mol. For both cavity polarizations, when the cavity frequencies $\omega_c \geq 2.5$ eV and the coupling strength $A_0 \geq 0.25$ a.u., the meta-substituted species is no longer the energetically favorable species and one can achieve the non-standard outcome (ortho- or para-substituted species). The experimental realizations of these

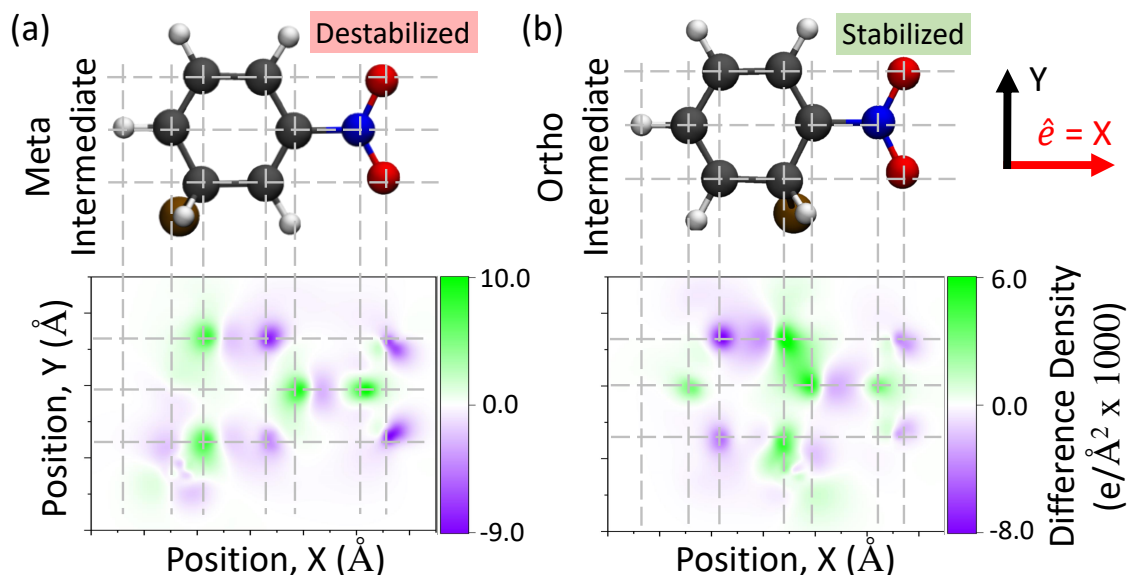


Figure 2: Ground state density difference $\Delta\rho_{00}(x, y) = \int dz[\rho_{00}(x, y, z) - \xi_{00}(x, y, z)]$ of (a) the meta-cationic intermediate and the ortho-cationic intermediate with a light-matter coupling strength $A_0 = 0.20$ a.u. and cavity frequency $\omega_c = 10.0$ eV. The cavity polarization is along the X-axis. The color bar indicates the magnitude and sign of the difference density $\Delta\rho_{00}(x, y)$, where positive (green) indicates electron charge accumulation and negative (purple) indicates electron charge depletion upon coupling the molecule with the cavity. Note that the color bar scales in panel (a) and panel (b) are different.

coupling conditions are possible using state-of-the-art plasmonic nano-cavity designs, with detailed discussions provided at the end of the paper in the **Experimental Relevance** section.

Overall, these results suggest that by coupling the nitrobenzene molecule to an optical cavity, the preferred bromination sites can be tuned to either ortho-substituted or para-substituted, whereas outside the cavity, only meta-substituted products are observed.²⁵ As such, coupling to the cavity allows obtaining the “impossible products” (para- and ortho-substituted PhNO₂-Br) outside the cavity.

To further understand these cavity-induced changes, we compute the ground state polaritonic density difference between the molecules coupled inside and outside the cavity (see Additional Methodology in the Supporting Information), which allows direct visualization of the cavity-mediated changes of the electron density of and interpret the relative stability of the various substituted reaction intermediates. The difference density function of the ground state is defined as, $\Delta\rho(X, Y, Z) = \rho_{00}(X, Y, Z) - \xi_{00}(X, Y, Z)$, where ρ_{00} is the polaritonic ground state electronic density (photonic DOFs have been traced out) and ξ_{00} is the bare electronic ground state density. Theoretical details for computing $\rho_{00}(X, Y, Z)$,

$\xi_{00}(X, Y, Z)$, and visualizations of $\Delta\rho(X, Y, Z)$ are provided in the Supporting Information. To help visualize the density difference, we further integrate out the Z-direction (perpendicular to the Benzene ring) and present the two-dimensional density difference surfaces $\Delta\rho(X, Y) = \int dZ\Delta\rho(X, Y, Z)$.

Fig. 2 present this density difference projected on the plane of the benzene ring when the cavity polarization is along $\hat{e} = \hat{X}$ (Scheme 1b, Fig. 1a) when $A_0 = 0.2$ a.u. and $\omega_c = 10$ eV. Under this coupling condition, the ortho cationic Wheland intermediate becomes more stable compared to the meta intermediate. Fig. 2a presents the two-dimensional density difference for the meta intermediate, and Fig. 2a presents for the ortho-substituted reaction intermediates. The color scheme of this plot is that the green color (positive values) indicates electronic charge accumulation and purple (negative values) indicates electronic charge depletion.

In Fig. 2a, one can see that the meta species exhibits both strongly atom-centered electron depletion and accumulation of electronic density. Upon coupling to the cavity, the electronic density migrates from both the oxygen atoms (purple color indicating a decrease in electron density) and the two ortho-carbons to the nitrogen atom (green color indicating an increase in electron density), its con-

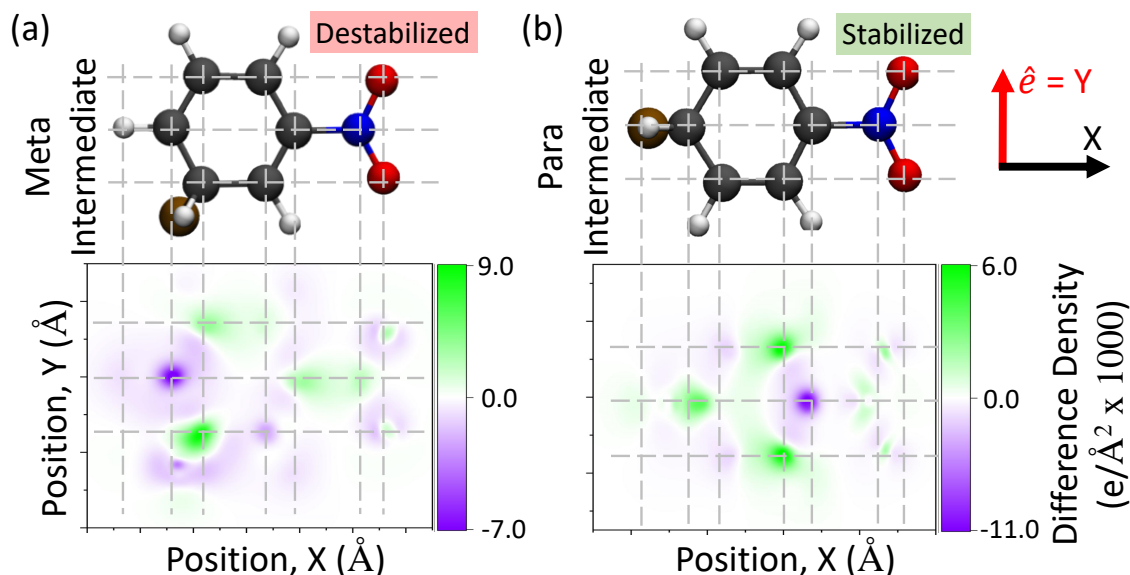


Figure 3: Ground state density difference $\Delta\rho_{00}(x, y) = \int dz[\rho_{00}(x, y, z) - \xi_{00}(x, y, z)]$ of (a) the meta-cationic Wheland intermediate and the para-cationic Wheland intermediate with a light-matter coupling strength $A_0 = 0.20$ a.u. and cavity frequency $\omega_c = 10.0$ eV. The cavity polarization is along the Y-axis. The color bar indicates the magnitude and sign of the difference density $\Delta\rho_{00}(x, y)$, where positive (green) indicates electron charge accumulation and negative (purple) indicates electron charge depletion upon coupling the molecule with the cavity. Note that the color bar scales in panel (a) and panel (b) are different.

necting carbon (*i.e.*, the nitrogen-connected carbon), and to both meta-carbons. It is interesting to note that the bromine itself shows charge rearrangement on its d_{z^2} orbital (see the three-dimensional isosurfaces for $\Delta\rho(X, Y, Z)$ in Fig. S4 and Fig. S5 in the **Supporting Information**), which may modify the bromine’s effectiveness to bond with its meta-carbon.

Fig. 2b presents the same plot for the ortho-substituted intermediate. Contrary to the largely atom-centered accumulation of charge in the meta species, the ortho species demonstrates a more delocalized charge accumulation (green color) across many carbon atoms (with lower intensity compared to the meta-substituted intermediate, see the scale of the color bar), where now the nitrogen-connected carbon as well as both ortho-carbons accumulate the majority of the charge. The nitrogen and the para-carbon accumulate some charge, but the delocalization across the three adjacent carbons, relative to the nitro group, allow for a lower-energy charge configuration compared to the charge-localized and largely repulsive electrostatic interaction (between the nitrogen-connected carbon and nitrogen atom), which was seen in the meta intermediate (Fig. 2a). We hypothesize that

the strong atom-centered accumulation of negative charge on the nitrogen-connected carbon and on the nitrogen atom is mainly responsible for destabilizing the meta-substituted intermediate inside the cavity, and the delocalized charge accumulation is the main reason for a more stable ortho-substituted species. These observations are similar at various other choices of coupling strength A_0 and cavity frequency ω_c (see Figs. S2 and Fig. S3 in the **Supporting Information**).

Fig. 3 presents the density difference map when cavity polarization is along the $\hat{e} = \mathbf{Y}$ direction, with $A_0 = 0.3$ a.u. and $\omega_c = 10$ eV. For this case, the para-substituted intermediate (Fig. 3b) is more stable than the meta-substituted intermediate (Fig. 3a), as shown in Fig. 1b). The corresponding isosurfaces as well as difference density maps for various coupling strengths are shown in Figs. S6-S9 in the **Supporting Information**. In this case, the meta species (Fig. 3a) exhibits charge accumulation at most of the atoms in the molecule, except for a significant charge depletion at the para-carbon and weakly depletion at the ortho-carbon on the bromine-side. Most importantly, the *bond between the carbon and nitrogen* accumulates electronic charge, which is in contrast to the previous

cases presented in Fig. 1. This charge accumulation between C-N destabilizes this intermediate due to the increased Coulomb repulsion between these atoms.

The para intermediate species presented in Fig. 3b exhibits a strongly localized charge depletion at the nitrogen-connected carbon as opposed to the charge accumulation in the meta species (Fig. 3a), *enabling the most stable structure of all the intermediate species observed* when couple the cavity with $\hat{\mathbf{e}} = \mathbf{Y}$. We hypothesize that this localized charge depletion is the main cause for a substantial energy reduction in terms of the relative energy compared to the meta position (see Fig. 1) due to the strongly delocalizing nature of charge distributions.

In addition, the symmetry of the density difference map for the para case is more apparent than in all of the previous cases (Fig. 2 and Fig. 3a), because the bromine attachment to ortho or meta positions induces a bias toward one side of the benzene ring. The para substitution provides additional symmetry, allowing for maximal charge separation between accumulated charge density (green color). The charge depletion, in the para case (Fig. 3b), is almost completely localized to the nitrogen-connected carbon, while in all other cases, the charge depletion is delocalized across the molecule. This delocalization of charge accumulation leads to further energetic stabilization of the para species.

Experimental Relevance.

The coupling strength required to observe such interesting changes to the ground state ($A_0 \approx 0.3$ a.u.) is much larger than the typical field strength in a Fabry-Pérot cavity. For a cavity frequency of $\omega_c = 1.8$ eV, this coupling strength converts into $\lambda = \sqrt{1/\epsilon\mathcal{V}} \approx 0.1$ a.u., consistent with the light-matter coupling strength used in the recent theoretical studies on cavity-enabled endo/exo selectivities of Diels-Alder reactions.¹⁴ Despite seeming to be large, recent experimental evidence suggests that these coupling strengths are achievable with state-of-the-art plasmonic nano-cavities. In these systems,^{26,27} the cavity mode volume is substantially reduced to the order of \AA^3 compared to the Fabry-Perot-type cavities whose volumes are on the order of μm^3 . The nano-cavity structure can achieve a record low mode volume²⁸ of $\mathcal{V} = 0.15$

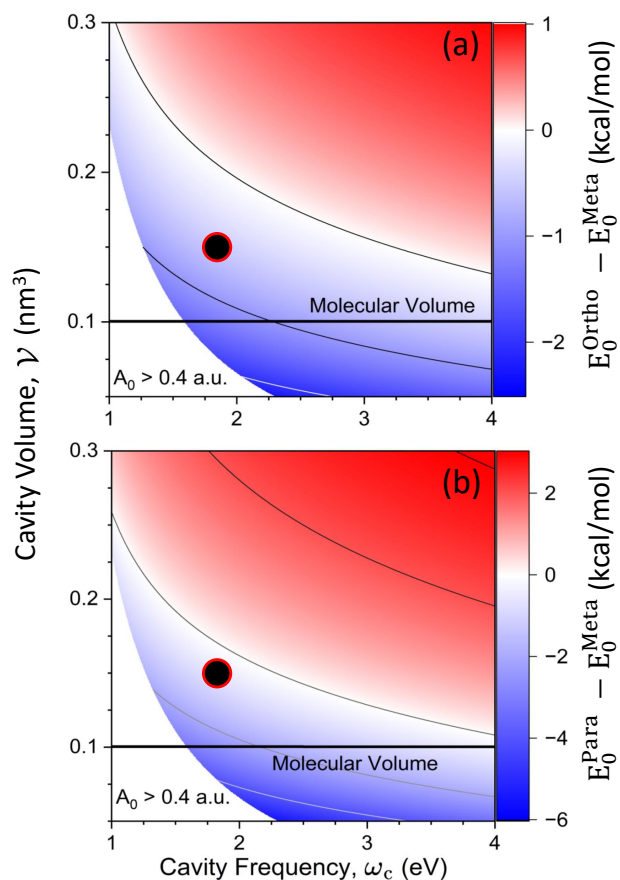


Figure 4: (a) Relative energy of the polaronic ground states between the ortho-intermediate and the meta-intermediate ($E_0^{\text{Ortho}}(\mathbf{R}) - E_0^{\text{Meta}}(\mathbf{R})$) when the cavity polarization $\hat{\mathbf{e}} = \mathbf{X}$. (b) Relative energy for the para-intermediate and the meta-intermediate ($E_0^{\text{Ortho}}(\mathbf{R}) - E_0^{\text{Meta}}(\mathbf{R})$), for $\hat{\mathbf{e}} = \mathbf{X}$. These relative energies are reported as functions of the cavity mode volume \mathcal{V} and cavity frequency ω_c . The color scales indicate the relative energy, with red showing thermodynamic favorability for the meta-substituted cation and blue for the other. The black circles correspond to a cavity volume of $\mathcal{V} = 0.15 \text{ nm}^3$ and a cavity frequency of $\omega_c = 1.8$ eV. This volume corresponds to $A_0 = 0.31$ a.u. and $\lambda = \sqrt{2\omega_c}A_0 = 0.11$ a.u.

nm^3 . Further, the state-of-the-art NanoParticle on Mirror (NPoM) cavity structure²⁹ can achieve a field intensity $\mathcal{E} = \omega_c A_0 \approx 2 \text{ V/nm}$.

To assess the experimental feasibility of the bromination reaction, Fig. 4a presents the relative energetics of the ortho- and meta-substituted intermediate $E_0^{\text{ortho}}(\mathbf{R}) - E_0^{\text{Meta}}(\mathbf{R})$ when the cavity polarization $\hat{\mathbf{e}} = \mathbf{X}$ (same data as presented in Fig. 1a) as a function of cavity frequency ω_c as

well as the cavity mode volume V (in the unit of nm^3). Fig. 4b presents the data the relative energetics of the para- and meta-substituted intermediate $E_0^{\text{Para}}(\mathbf{R}) - E_0^{\text{Meta}}(\mathbf{R})$ when $\hat{\mathbf{e}} = \mathbf{Y}$ (same data as presented in Fig. 1b). Here, we focus on the range of frequency $\omega_c \approx 1 \sim 4$ which is within the typical range of nano-cavity. The cavity frequency of the NPoM cavity depends on the materials of the nanoparticle, the size of the nanoparticle, and the gap size between the particle and the mirror surface. The typical value is for gold nano-particle about $\omega_c \approx 2$ eV (600 nm), silver nano-particle about $\omega_c \approx 2.5$ eV (500 nm) and aluminum nano-particle about $\omega_c \approx 3$ eV (400 nm).¹⁸ In particular, for the recent experiments^{26,27} on a single emitter strongly coupled to the plasmonic nano-cavity, with gold nano-particle the cavity has a frequency of $\omega_c = 1.8$ eV. With the currently possible mode volume $\mathcal{V} = 0.15 \text{ nm}^3$, the equivalent coupling strength is $A_0 = 0.3$ a.u. (or $\lambda = 0.1$ a.u.) and field intensity is $\mathcal{E} = 10.9$ V/nm. With these parameters, one can lower the energy of ortho-intermediate by 0.49 kcal/mol compared to the meta intermediate (for $\hat{\mathbf{e}} = \mathbf{X}$) and lower the energy of para-intermediate by 0.45 kcal/mol compared to the meta intermediate (for $\hat{\mathbf{e}} = \mathbf{Y}$). Although the non-meta complexes only have a slightly lower energies, these realistic coupling strengths already start to favor the ortho or para products and one should expect to obtain the mixtures of these products together with the meta-substituted product.

For the single molecule strong coupling case, one often has to control the molecular orientation with respect to the cavity field polarization direction. For example, recent theoretical work suggests that when coupling the cavity to particular directions, one can selectively obtain the endo- or the exo-products of a Diels-Alder reaction,¹⁴ whereas an isotropic random orientation of the molecule will likely end up giving an equal mixture of both configurations, a situation similar to outside the cavity case. Experimentally, one can control the molecular orientations to align the cavity field for single molecule-NPoM cavity using super-molecular chemistry.²⁶ Nevertheless, perfectly controlling the molecular orientation might be challenging. The currently proposed bromination reaction, on the other hand, does not require precise control of the orientation of molecules, if the goal is to obtain non-meta-substituted products in order to demonstrate the cavity-controlled reaction and generate a new product. This is because when the cavity

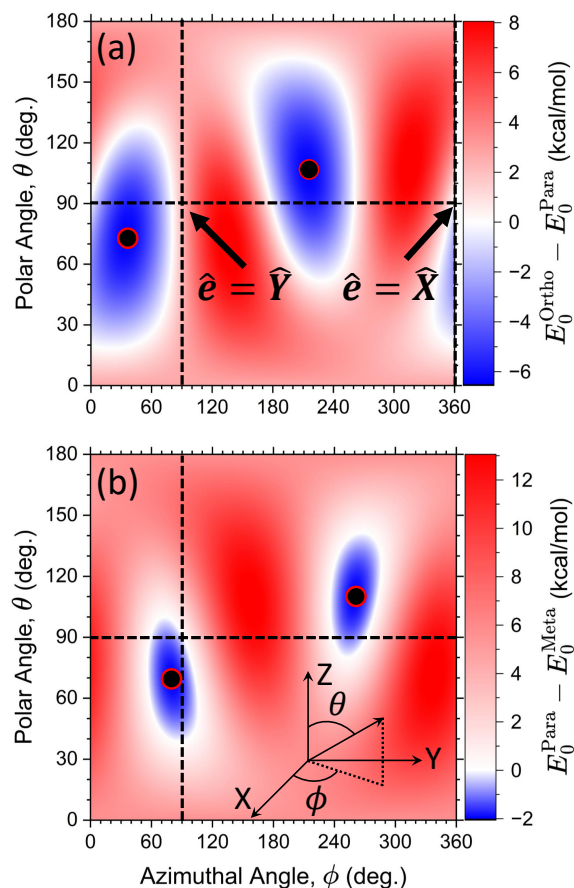


Figure 5: Relative energy of the polaritonic ground states between (a) ortho-PhNO₂-Br⁺ and meta-PhNO₂-Br⁺ and (b) para-PhNO₂-Br⁺ and meta-PhNO₂-Br⁺, as a function of the azimuthal $\theta \in [0, 2\pi)$ and polar $\phi \in [0, \pi)$ angles of the cavity polarization vector with respect to the molecular cartesian axes (defined in Scheme 1a and further in the inset of panel (b) of Fig. 5). The cavity frequency and coupling strength are fixed at $\omega_c = 1.8$ eV and $A_0 = 0.3$ a.u. (cavity volume $\mathcal{V} = 0.15 \text{ nm}^3$). The minimum Values of the relative energies in each case are (a) -1.97 kcal/mol and (b) -6.43 kcal/mol, which are denoted by the black circles.

polarizes along \mathbf{X} direction, the ortho product is preferred, and when the cavity polarizes along \mathbf{Y} direction, the para product is preferred. When the cavity polarizes along \mathbf{Z} direction because the dipole along the direction perpendicular to the benzene ring is nearly zero ($\hat{\boldsymbol{\mu}} \cdot \mathbf{Z} \approx 0$), the cavity does not couple to the molecule, and we expect the product to be meta-substituted (same as outside the cavity). As such, randomly orientated molecules strongly coupled to the nano-cavity will gener-

ate new products (ortho- and para-substituted nitrobenzene) that are completely different compared to the reaction outside the cavity (which only yields the meta-substituted nitrobenzene). On the other hand, if the objective is to only obtain either ortho- or para-substituted species, then one would either need to control molecular orientation along the cavity field polarization, which, as stated above, has been accomplished in recent experimental works,²⁶ or separate the mixture of products post-reaction.

To theoretically confirm this hypothesis, we also performed a full scan of all possible spacial orientations of the molecule with respect to the cavity polarization direction, with the results presented in Fig. 5. Here, we focus on a gold nanoparticle plasmonic cavity with $\omega = 1.8$ eV, and mode volume $\mathcal{V} = 0.15$ nm³ (field strength $\mathcal{E} = 10.8$ V/nm.¹⁸ The cavity polarization direction $\hat{\mathbf{e}}$ with respect to the \mathbf{X} , \mathbf{Y} , and \mathbf{Z} directions of the molecule can be characterized by the polar angle θ and the azimuthal angle ϕ (see inset of Fig. 5b).

Fig. 5a presents the results of $E_0^{\text{Ortho}}(\mathbf{R}) - E_0^{\text{Meta}}(\mathbf{R})$ and Fig. 5b presents the results of $E_0^{\text{Para}}(\mathbf{R}) - E_0^{\text{Meta}}(\mathbf{R})$. When $\theta = 90^\circ$ and $\phi = 0^\circ$, $\hat{\mathbf{e}} = \mathbf{X}$ (corresponding to Fig. 1a with $\omega_c = 1.8$ eV and $A_0 = 0.3$ a.u.) and when $\theta = 90^\circ$ and $\phi = 90^\circ$, $\hat{\mathbf{e}} = \mathbf{Y}$ (corresponding to Fig. 1a with $\omega_c = 1.8$ eV and $A_0 = 0.3$ a.u.). On one hand, when $\theta = 0^\circ$ for $\hat{\mathbf{e}} = \mathbf{Z}$ or $\theta = 180^\circ$ for $\hat{\mathbf{e}} = -\mathbf{Z}$, the cavity polarization is along Z direction where the molecular dipole is nearly zero, and the cavity modification diminishes, as we expected. On the other hand, the most stable energy for the ortho-substituted complex is achieved when $\theta \sim 75^\circ$ and $\phi \sim 40^\circ$, which is ~ 6.4 kcal/mol more stable compared to meta-substituted complex. The most stable energy for the para-substituted complex is achieved when $\theta = 80^\circ$ and $\phi = 70^\circ$, which is ~ 2.0 kcal/mol more stable compared to meta-substituted complex. From this figure, we can see the region of θ and ϕ where ortho- or para-substituted intermediate is more stable than meta-substituted configuration. So long as the molecule can access these spacial region, one should expect that coupling to cavity can generate non-meta product.

Conclusions.

In this work, we use the *ab initio* cavity Quantum Electrodynamics approach to investigate a chemical reaction, the bromination of nitrobenzene, coupled to an optical cavity. Our approach is based

on the previously developed parametrized QED (pQED) method, which uses the QED Pauli-Fierz Hamiltonian to describe light and matter interactions and uses adiabatic electronic states and all dipole matrix elements between them as input to compute the polariton eigenenergies.¹⁶

The bromination of nitrobenzene outside of a cavity exhibits only one possible product, which is the meta-substituted 1-bromo-3-nitrobenzene. Upon coupling to the cavity, we calculate the relative energies of the meta-, ortho-, and para-substituted catatonic active complexes $\text{PhNO}_2\text{-Br}^+$, which are the well-known key intermediates that dictate the outcome of the reaction. Outside the cavity, the meta-substituted intermediate is 2 kcal/mol lower than the ortho-substituted intermediate and about 5 kcal/mol lower than the ortho-substituted intermediate, in agreement with the well-known experimental results that the only observed product is the meta-substituted nitrobenzene.

Upon coupling to the cavity and aligning the cavity polarization direction along the X-axis (see Scheme. 1a), the ortho-substituted intermediate is energetically more stable than the meta-substituted intermediate by up to 4 kcal/mol with the cavity frequency and the coupling strength we scanned. When the cavity polarization direction is along the Y-axis (see Scheme. 1b), the para-substituted intermediate is energetically more stable than the meta-substituted intermediate, with up to -15 kcal/mol. These changes in the favorability of the various substituted intermediates are due to the quantum light-matter interactions between the molecules and cavity, which mixes the character of electronic excited states into the polariton ground state. These changes are characterized using the electronic density difference of the system inside and outside the cavity. We thus have theoretically shown that one can obtain ortho- or para-substituted nitrobenzene when coupling the reaction to an optical cavity, generating new products that otherwise would not appear in the same reaction outside the cavity.

To further probe the possibility of experimental realization of our theoretical prediction, we focus on the currently available plasmonic nanocavity parameters for the cavity frequency and field strength. In particular, we choose $\omega_c = 1.8$ eV and the coupling strength $A_0 = 0.3$ a.u. (or $\lambda = 0.1$ a.u.) which corresponding to a mode volume $\mathcal{V} =$ and field intensity of $\mathcal{E} = 10.8$ V/nm.

We further scanned all possible polarization directions. Interestingly, we can find finite region in the configuration space of polar angle and azimuthal angle which make the ortho- or para-substituted species more stable than the para-substituted active complex, with the largest stabilization energy of 6.43 kcal/mol for ortho and 1.97 kcal/mol for para. This implies that with the nano-cavity, and fully isotropic orientations of the molecule inside, one should expect to generate a non-meta substituted product, and demonstrating that coupling to cavity can make the non-standard product which can not be easily obtained otherwise. This work demonstrates the possibility of polariton-mediated changes to local chemistry. The theoretical prediction can, in principle, be experimentally verified using state-of-the-art plasmonic nano-cavity designs.

Theoretical Methods.

We use the *ab initio* polariton approach we developed in the previous work, which we refer to as the parametrized-QED (pQED) approach.¹⁶ The pQED approach uses Pauli-Fierz Hamiltonian in the Born-Oppenheimer approximation (see Eq. 1) to describe light and matter interactions and use adiabatic electronic states as the basis for the electronic degrees of freedom, and Fock states as the basis for the photonic DOF.

The polariton eigenstates and eigenenergies are obtained by solving the following equation

$$\hat{H}_{\text{PF}}|\Phi_j(\mathbf{R})\rangle = E_j(\mathbf{R})|\Phi_j(\mathbf{R})\rangle, \quad (3)$$

where \hat{H}_{PF} is given in Eq. 1, $E_j(\mathbf{R})$ is the Born-Oppenheimer polaritonic potential energy surfaces (which parametrically depend on the nuclear coordinates \mathbf{R}), and $|\Phi_j(\mathbf{R})\rangle$ is the polariton state. We directly diagonalize the polaritonic Hamiltonian \hat{H}_{PF} matrix and obtain the eigenvalues. The basis is constructed using the tensor product of electronic adiabatic states $|\psi_\alpha(\mathbf{R})\rangle$ (*i.e.*, eigenstates of the electronic Hamiltonian \hat{H}_{el}) and the Fock states $|n\rangle$ (*i.e.*, eigenstates of the photonic Hamiltonian \hat{H}_{ph}), expressed as $|\psi_\alpha(\mathbf{R})\rangle \otimes |n\rangle \equiv |\psi_\alpha(\mathbf{R}), n\rangle$. This basis is used to evaluate the matrix elements of \hat{H}_{PF} , and diagonalizing it provides $E_j(\mathbf{R})$ and the corresponding polariton states

$$|\Phi_j(\mathbf{R})\rangle = \sum_{\alpha} \sum_n^{N_{\text{el}} N_{\text{F}}} C_{\alpha n}^j |\psi_\alpha(\mathbf{R}), n\rangle, \quad (4)$$

where $C_{\alpha n}^j = \langle \psi_\alpha(\mathbf{R}), n | \Phi_j(\mathbf{R}) \rangle$. Here, the number of included electronic states, N_{el} , and photonic Fock/number states, N_{F} , are treated as convergence parameters. A convergence test is provided in the **Supporting Information**, and the typical numbers of states are $N_{\text{F}} = 5$ and $N_{\text{el}} = 50$. Further details regarding the pQED approach are provided in the **Supporting Information**. The accuracy of the above-described pQED approach has been benchmarked¹⁶ with the more accurate coupled-cluster QED (CC-QED) approach, where the pQED method generates nearly quantitative agreement with the CC-QED approach.

All electronic structure calculations were performed using the QCHEM software package³⁰ using linear response time-dependent density functional theory (LR-TD-DFT) using the ω B97XD hybrid exchange-correlation functional with the 6-311+G* basis set. The geometries of the PhNO₂-Br⁺ intermediate with various substitution positions are optimized in its electronic ground states. When the cavity polarization direction $\hat{\mathbf{e}}$ is aligned with a particular axis (*e.g.*, $\hat{\mathbf{e}} = \mathbf{X}$ or $\hat{\mathbf{e}} = \mathbf{Y}$ in Fig. 1), the matrix elements $\langle \psi_\alpha | \hat{\boldsymbol{\mu}} \cdot \mathbf{X} | \psi_\gamma \rangle$ and $\langle \psi_\alpha | \hat{\boldsymbol{\mu}} \cdot \mathbf{Y} | \psi_\gamma \rangle$ are used as the input for the light-matter interaction term $\hat{\boldsymbol{\mu}} \cdot \hat{\mathbf{e}}$ as well as for the DSE term. For the cavity polarization direction $\hat{\mathbf{e}}$ with respect to the \mathbf{X} , \mathbf{Y} , and \mathbf{Z} directions of the molecule (see inset of Fig. 5b), the interaction term is $\hat{\mathbf{e}} \cdot \hat{\boldsymbol{\mu}} = \sin \theta \cos \phi \mathbf{X} \cdot \hat{\boldsymbol{\mu}} + \sin \theta \sin \phi \mathbf{Y} \cdot \hat{\boldsymbol{\mu}} + \cos \theta \mathbf{Z} \cdot \hat{\boldsymbol{\mu}}$. The electronic excited state energies and the molecular transition dipole matrix were computed using the QCHEM package.³⁰

Acknowledgement This work was supported by the National Science Foundation’s “Center for Quantum Electrodynamics for Selective Transformations (QuEST)” under the grant number CHE-2124398. P.H. appreciates the support of the Cottrell Scholar Award (a program by the Research Corporation for Science Advancement). Computing resources were provided by the Center for Integrated Research Computing (CIRC) at the University of Rochester. We appreciate the helpful discussions with Arkajit Mandal, Yu Zhang, Jonas Widness, Julianna Mouat, and Rachel Bangle.

Supporting Information Available

Additional figures that support the discussion in the main text are provided, namely three-dimensional isosurfaces of the difference density as well as figures that showcase the expansion of the photonic ground state density in the basis of electronic excited state densities and transition densities. Further methodological details are also provided.

References

- (1) Zeng, H.; Pérez-Sánchez, J. B.; Eckdahl, C. T.; Liu, P.; Chang, W. J.; Weiss, E. A.; Kalow, J. A.; Yuen-Zhou, J.; Stern, N. P. Control of Photoswitching Kinetics with Strong Light–Matter Coupling in a Cavity. *J. Am. Chem. Soc.* **2023**,
- (2) Hutchison, J. A.; Schwartz, T.; Genet, C.; Devaux, E.; Ebbesen, T. W. Modifying Chemical Landscapes by Coupling to Vacuum Fields. *Angew. Chem. Int. Ed.* **2012**, *51*, 1592–1596.
- (3) Lather, J.; Bhatt, P.; Thomas, A.; Ebbesen, T. W.; George, J. Cavity Catalysis by Cooperative Vibrational Strong Coupling of Reactant and Solvent Molecules. *Angew. Chem. Int. Ed.* **2019**, *58*, 10635–10638.
- (4) Lather, J.; Thabassum, A. N. K.; Singh, J.; George, J. Cavity catalysis: modifying linear free-energy relationship under cooperative vibrational strong coupling. *Chem. Sci.* **2022**, *13*, 195–202.
- (5) Thomas, A.; George, J.; Shalabney, A.; Dryzhakov, M.; Varma, S. J.; Moran, J.; Chervy, T.; Zhong, X.; Devaux, E.; Genet, C.; Hutchison, J. A.; Ebbesen, T. W. Ground-State Chemical Reactivity under Vibrational Coupling to the Vacuum Electromagnetic Field. *Angew. Chem. Int. Ed.* **2016**, *55*, 11462–11466.
- (6) Thomas, A.; Jayachandran, A.; Lethuillier-Karl, L.; Vergauwe, R. M. A.; Nagarajan, K.; Devaux, E.; Genet, C.; Moran, J.; Ebbesen, T. W. Ground state chemistry under vibrational strong coupling: dependence of thermodynamic parameters on the Rabi splitting energy. *Nanophotonics* **2020**, *9*, 249–255.
- (7) Thomas, A.; Lethuillier-Karl, L.; Nagarajan, K.; Vergauwe, R. M. A.; George, J.; Chervy, T.; Shalabney, A.; Devaux, E.; Genet, C.; Moran, J.; Ebbesen, T. W. Tiltting a ground-state reactivity landscape by vibrational strong coupling. *Science* **2019**, *363*, 615–619.
- (8) Flick, J.; Schäfer, C.; Ruggenthaler, M.; Appel, H.; Rubio, A. Ab Initio Optimized Effective Potentials for Real Molecules in Optical Cavities: Photon Contributions to the Molecular Ground State. *ACS Photonics* **2018**, *5*, 992–1005.
- (9) Haugland, T. S.; Ronca, E.; Kjønstad, E. F.; Rubio, A.; Koch, H. Coupled Cluster Theory for Molecular Polaritons: Changing Ground and Excited States. *Phys. Rev. X* **2020**, *10*, 041043.
- (10) Mordovina, U.; Bungey, C.; Appel, H.; Knowles, P. J.; Rubio, A.; Manby, F. R. Polaritonic coupled-cluster theory. *Phys. Rev. Research* **2020**, *2*, 023262.
- (11) DePrince, A. E. Cavity-modulated ionization potentials and electron affinities from quantum electrodynamics coupled-cluster theory. *J. Chem. Phys.* **2022**, *154*, 094112.
- (12) Riso, R. R.; Haugland, T. S.; Ronca, E.; Koch, H. Molecular orbital theory in cavity QED environments. *Nat. Commun.* **2022**, *13*, 1368.
- (13) Pavošević, F.; Hammes-Schiffer, S.; Rubio, A.; Flick, J. Cavity-Modulated Proton Transfer Reactions. *J. Am. Chem. Soc.* **2022**, *144*, 4995–5002.
- (14) Pavošević, F.; Smith, R. L.; Rubio, A. Computational study on the catalytic control of endo/exo Diels-Alder reactions by cavity quantum vacuum fluctuations. *Nat Commun* **2023**, *14*, 2766.
- (15) Weight, B. M.; Tretiak, S.; Zhang, Y. A Diffusion Quantum Monte Carlo Approach to the Polaritonic Ground State. **2023**, arXiv:2309.02349.

- (16) Weight, B. M.; Krauss, T. D.; Huo, P. Investigating Molecular Exciton Polaritons Using Ab Initio Cavity Quantum Electrodynamics. *J. Phys. Chem. Lett.* **2023**, *14*, 5901–5913.
- (17) Pavosevic, F.; Smith, R. L.; Rubio, A. Cavity Click Chemistry: Cavity-Catalyzed Azide-Alkyne Cycloaddition. 2023; <http://arxiv.org/abs/2305.09496>.
- (18) Akselrod, G. M.; Huang, J.; Hoang, T. B.; Bowen, P. T.; Su, L.; Smith, D. R.; Mikkelsen, M. H. Large-Area Metasurface Perfect Absorbers from Visible to Near-Infrared. *Advanced Materials* **2015**, *27*, 8028–8034.
- (19) Mandal, A.; Taylor, M. A. D.; Huo, P. Theory for Cavity-Modified Ground-State Reactivities via Electron–Photon Interactions. *J. Phys. Chem. A* **2023**, *127*, 6830–6841.
- (20) Mandal, A.; Taylor, M. A. D.; Weight, B. M.; Koessler, E. R.; Li, X.; Huo, P. Theoretical Advances in Polariton Chemistry and Molecular Cavity Quantum Electrodynamics. **2023**, *123*, 9786–9879.
- (21) Taylor, M. A. D.; Mandal, A.; Zhou, W.; Huo, P. Resolution of Gauge Ambiguities in Molecular Cavity Quantum Electrodynamics. *Phys. Rev. Lett.* **2020**, *125*, 123602.
- (22) Mandal, A.; Vega, S. M.; Huo, P. Polarized Fock States and the Dynamical Casimir Effect in Molecular Cavity Quantum Electrodynamics. *J. Phys. Chem. Lett.* **2020**, *11*, 9215–9223.
- (23) Rokaj, V.; Welakuh, D. M.; Ruggenthaler, M.; Rubio, A. Light–matter interaction in the long-wavelength limit: no ground-state without dipole self-energy. *J. Phys. B: At. Mol. Opt. Phys.* **2018**, *51*, 034005.
- (24) Jaynes, E. T.; Cummings, F. W. Comparison of quantum and semiclassical radiation theories with application to the beam maser. *Proc. IEEE* **1963**, *51*, 89–109.
- (25) Loudon, M.; Parise, J. *Organic Chemistry*; Macmillan Learning, 2015.
- (26) Chikkaraddy, R.; de Nijs, B.; Benz, F.; Barrow, S. J.; Scherman, O. A.; Rosta, E.; Demetriadou, A.; Fox, P.; Hess, O.; Baumberg, J. J. Single-molecule strong coupling at room temperature in plasmonic nanocavities. *Nature* **2016**, *535*, 127–130.
- (27) Santhosh, K.; Bitton, O.; Chuntunov, L.; Haran, G. Vacuum Rabi splitting in a plasmonic cavity at the single quantum emitter limit. *Nat. Commun.* **2016**, *7*, 1–5.
- (28) Wu, T.; Yan, W.; Lalanne, P. Bright Plasmons with Cubic Nanometer Mode Volumes through Mode Hybridization. *ACS Photonics* **2021**, *8*, 307–314.
- (29) Chen, S.; Xiao, Y.-H.; Qin, M.; Zhou, G.; Dong, R.; Devasenathipathy, R.; Wu, D.-Y.; Yang, L. Quantification of the Real Plasmonic Field Transverse Distribution in a Nanocavity Using the Vibrational Stark Effect. *J. Phys. Chem. Lett.* **2023**, *14*, 1708–1713.
- (30) Epifanovsky, E. et al. Software for the frontiers of quantum chemistry: An overview of developments in the Q-Chem 5 package. *J. Chem. Phys.* **2021**, *155*, 084801.